6th World Congress on Structural and Multidisciplinary Optimization
Rio de Janeiro, Brazil, 30 May - 03 June 2005

Optimal Shape Design and its application to microstructures

E. Friedmann[1]

(1) Interdisciplinary Center for Scientific Computing, University of Heidelberg, Germany, friedmann@iwr.uni-heidelberg.de

1. Abstract
Previous research has established that a smooth surface has not the minimal drag. As a result of many experiments which have been carried out by different laboratories (e.g. NASA, DLR Berlin) a surface with tiny grooves aligned in the streamwise direction was proposed as a drag reduction device. The aim of this project is to find the optimal shape of such microstructures on surfaces of submerged bodies. We assume that these microstructures remain in the viscous sublayer which is described by the 3D incompressible, steady-state Navier-Stokes equation with a Couette Flow profile. The objective function of our optimization problem is the tangential drag force, which we want to minimize. Solving this problem is difficult because of the oscillating boundary, which causes a big amount of data. We apply Homogenization theory and replace the rough boundary by a smooth artificial one, where the right boundary conditions have been determined. Furthermore, our optimization problem can be simplified using this approximation and we end up minimizing the Navier constant, which depends only on the velocity of an auxiliary boundary layer equation. To solve the optimization problem we consider the sensitivity. From the results obtained here, we are able to derive the necessary optimality condition and to construct a sequence of admissible domains which tends to the optimal solution. We use gradient based optimization methods and the finite element method on unstructured grids for the numerics of state equation. The results obtained with this approach give us a drag reduction of approximately 2-6% relative to the drag of the smooth configuration.
2. Keywords: drag minimization, shark skin, Couette flow, homogenization.

3. Introduction

For the last decade we can observe an increasing scientific interest in fluid dynamic effects caused by biological surfaces like Lotus leaves and shark skin. In both examples microstructures on the surface play an important role. As sharks belong to some of the oldest animals in nature they have optimized their shape for more than 200 million years, i.e. to minimize the energy consumption during movement, to reduce drag. On the skin of fast swimming sharks certain microstructures were found. The scales are tiny (0.2-0.5mm) and the ridges are in the streamwise direction. Their number is between 3 and 7 ridges on one scale of a fast shark. Calculated with the body length the Reynolds number of a fast shark is high ($\mathrm{Re} \approx 10^6 - 10^7$). Different laboratories tested artificial surfaces with this kind of scales in a turbulent boundary layer, and found a drag reduction of about 7%. Examples for applications are fuel saving in the flight industry and drag minimization in sports competitions (yachting, swimming, cycling). A fluid dynamical explanation why riblets reduce drag is given by many authors, e.g. Bechert, Bartenwerfer, Hoppe, Reif, see [1], [3]. We will focus in this work on how the shape of microstructures should look like to reduce skin friction.
It is not new, that a blade like structure has a lower drag than other structures with the same height. Our calculations are in agreement with results obtained in the experimental works done by Bechert, Walsh and others, where shapes of microstructures were compared ([1], [2]). So far no optimization problems were considered to improove the shape of microstructures. To be able to solve the optimization problem whithout special and too expensive numerical methods we have to combine shape design and homogenization and we will see how much this theory facilitates our numerical calculations. From the calculations in one cell, a very small part of the total geometry, we can conclude through scaling to the drag of the whole rough channel.

4. The viscous sublayer in two dimensions

To model the flow over microstructures we consider at first the boundary layer of a turbulent flow which consists of the flow within a thin layer. This layer consists of three parts: a relative small viscous sublayer, the middle buffer layer and the logarithmic layer. The riblets used on the surface of aircrafts

extend into the buffer layer. With this kind of riblets a drag reduction of about 8-10% was obtained in experiments. Analysis of flow within the buffer layer is still out of reach. Our model is restricted to riblets in the viscous sublayer of the turbulent boundary layer.
The flow in this viscous sublayer of height δ is the same flow considered between two parallel plates in a distance δ, where the lower plate is kept fix and the upper one moves with velocity U uniformly and parallel to the lower one. Due to this parallel moving the transverse velocity component in y-direction is zero. Because of the adherence of the fluid to the surfaces a linear velocity distribution between the two plates, the so called Couette flow, describes the model. The boundary layer thickness and the velocity component parallel to the surface are independent of x, they do not vary along the wall.
Our model describes the flow in a two dimensional channel $P = (0, L_1) \times (0, L_2)$ of height of the viscous sublayer $L_2 = \delta = 10^{-3}$ m with a rough surface bottom, the so-called layer of roughness $\mathcal{R}^\varepsilon = (\cup\varepsilon(Y + (k_1, -b_2))) \cap ((0, L_1) \times (-\varepsilon b_2, 0))$ which consists of the periodically repetition of one cell of roughness $Y = \{y \in Z = (0, b_1) \times (0, b_2) \mid\ b_2 > y_2 > max\{0, \gamma(y_1)\}\}$. The rough boundary is denoted by $\mathcal{B}^\varepsilon = \varepsilon(\cup\gamma + (k_1, -b_2))$ and describes periodically distributed humps of characteristic length and amplitude. The domain where the fluid flows is thus given by $\Omega^\varepsilon = P \cup \Sigma \cup \mathcal{R}^\varepsilon$. The flow itself can be described with the incompressible steady state Navier Stokes equations with a Couette flow profile (Re=1) with Dirichlet boundary conditions on the rough boundary, the so-called no-slip condition:

$$\begin{cases} \mu\Delta v^\varepsilon + (v^\varepsilon\nabla)v^\varepsilon + \nabla p^\varepsilon &= 0, \text{ in } \Omega^\varepsilon \\ \text{div } v^\varepsilon &= 0, \text{ in } \Omega^\varepsilon \\ v^\varepsilon &= 0, \ \mathcal{B}^\varepsilon \\ v^\varepsilon &= U, \ \Sigma_2 \\ \{v^\varepsilon, p^\varepsilon\} &- \ x_1 \text{ periodic.} \end{cases} \tag{1}$$

To compute the solution $\{v^\varepsilon, p^\varepsilon\}$ of this system numerically is difficult. Because of the rough boundary we need a huge amount of data and a very fine mesh to capture the oscillating boundary as exact as possible. To reduce the numerical effort we first apply homogenization, where the rough boundary is replaced by a smooth one with artificial boundary conditions as proposed by Jäger and Mikelić in [6], the so-called Navier slip condition. The the effective equations are calculated by the authors as a limit process, where the characteristic lenght ε tends to zero. We will use the results from [5] and [6] in order to approximate our oscillating system (1) in the next section.

4.1. Homogenization applied to the incompressible steady state Navier Stokes equation in the viscous sublayer
The Couette flow in P, satisfying the no-slip condition at Σ, is given by

$$v^0 = \frac{Ux_2}{L_2}, \qquad p^0 = 0. \tag{2}$$

The idea of the authors from [6] was to extend the velocity v^0 to $\Omega^\varepsilon \setminus P$ by zero and to construct the solution of (1) as a small perturbation to the Couette flow.

Theorem 1 *Let $|U|L_2 < 2\nu$ and let*

$$R_0 = \frac{\nu}{L_2} \frac{|U|}{\nu - \frac{L_2|U|}{2}} \sqrt{L_1 b_2}. \tag{3}$$

Then for $\varepsilon < \frac{L_2}{b_2}$ the problem (1) has a solution $\{v^\varepsilon, p^\varepsilon\} \in H^2(\Omega^\varepsilon)^2 \times H^1(\Omega^\varepsilon)$, εb_1 - periodic in x_1 and satisfying

$$||\nabla(v^\varepsilon - v^0)||_{L^2(\Omega^\varepsilon)^4} \leq R_0\sqrt{\varepsilon}. \tag{4}$$

Moreover,

$$||v^\varepsilon||_{L^2(\Omega^\varepsilon \setminus P)^2} \leq \frac{b_2}{\sqrt{2}} R_0 \varepsilon\sqrt{\varepsilon} \tag{5}$$

$$||v^\varepsilon||_{L^2(\Sigma)^2} \leq 2^{\frac{1}{4}}\sqrt{b_2}R_0\varepsilon, \tag{6}$$

$$||p^\varepsilon - p^0||_{L^2(P)} \leq C\sqrt{\varepsilon}. \tag{7}$$

Furthermore, the solution is C^∞ in P.

Proof. see [6].

Theorem 2 *Let $|U|L_2 \leq \nu$ and $\varepsilon \leq C(b_1, b_2, L_1)\nu^{\frac{9}{14}}$. Then $v^\varepsilon \in H^2(\Omega^\varepsilon)$, constructed in Theorem 1, is the unique solution to (1) and $p^\varepsilon \in H^1(\Omega^\varepsilon)$ is unique up to a constant.*

Proof. see [6].
The solution $\{v^\varepsilon, p^\varepsilon\}$ was constructed formal as a rigorously asymptotic expansion. The effective equations are obtained through a limit process of this asymptotic expansion for $\varepsilon \to 0$. It is clear that in P, far away from the irregularities, the flow will not be influenced much. It will still be governed by the incompressible steady state Navier-Stokes system. The presence of the irregularities will only contribute to the effective boundary conditions at the artificial smooth boundary S. This contribution is found exactly in the Navier's slip condition, in the coefficient C^{bl}, the so-called Navier constant. This constant is calculated using an auxiliary boundary layer equation as outlined later.
The effective Couette Navier flow is given by:

$$\begin{cases} -\nu\Delta u^{\text{eff}} + (u^{\text{eff}}\nabla)u^{\text{eff}} + \nabla p^{\text{eff}} &= 0, \quad P \\ \text{div } u^{\text{eff}} &= 0, \quad P \\ u^{\text{eff}} &= (U_1, 0), \quad \Sigma_2 \\ u_1^{\text{eff}} &= -\varepsilon C^{\text{bl}} \frac{\partial u_i^{\text{eff}}}{\partial x_2}, \quad S \\ u_2^{\text{eff}} &= 0, \quad S \\ \{u^{\text{eff}}, p^{\text{eff}}\} \quad x_1 &- \text{ periodic}, \end{cases} \tag{8}$$

Proposition 3 *If $|U|L_2 < 2\nu$, then the unique solution of (8) is given by:*

$$\begin{cases} u^{\text{eff}} &= (U + (\frac{x_2}{L_2} - 1)(1 - \frac{\varepsilon}{L_2}C^{\text{bl}})^{-1}U, 0), \quad \textit{in } P \\ p^{\text{eff}} &= 0, \quad \textit{in } P. \end{cases} \tag{9}$$

Proof. see [6].
Further we would like to replace $\{v^\varepsilon, p^\varepsilon\}$ by $\{u^{\text{eff}}, p^{\text{eff}}\}$. Therefore we have to mention the error estimates made in this process from [6]:

Corollary 4 *Under the assumptions of theorem 1 we have*

$$||\nabla(v^\varepsilon - u^{eff})||_{L^1(P)} \leq C\varepsilon, \tag{10}$$

$$\sqrt{\varepsilon}||v^\varepsilon - u^{eff}||_{L^2(P)} + ||v^\varepsilon - u^{eff}||_{L^1(P)} \leq C\varepsilon^2. \tag{11}$$

4.2. Which microstructure is better? - A shape optimization problem
We want to analyze the effect of the microstructures on the drag. The normalized tangential drag force on S is given by

$$\mathcal{F}_t^\varepsilon = \frac{1}{L_1}\int_S \nu n \cdot \sigma \cdot e_1 dx_1 = \frac{1}{L_1}\int_S \frac{1}{2}\nu\Big(\frac{\partial}{\partial x_2}u_1^\varepsilon(x_1, 0) + \frac{\partial}{\partial x_1}u_2^\varepsilon(x_1, 0)\Big)dx_1, \tag{12}$$

where $n = e_2$ is the normal vector to S and $\sigma_{ij} = \frac{1}{2}(\frac{\partial u_i}{\partial x_j} + \frac{\partial u_j}{\partial x_i}) - p\delta_{ij}$ is the total stress tensor, consisting of the viscous shear stress and of the fluid pressure p. In the last section we have seen that we are

able to approximate $\{v^\varepsilon, p^\varepsilon\}$ by $\{u^{\text{eff}}, p^{\text{eff}}\}$ in order to reduce the calculation costs. With these effective parameters the so-called effective tangential drag force is given by

$$\mathcal{F}_t^{\text{eff}} = \frac{1}{L_1}\int_S \frac{1}{2}\nu\Big(\frac{\partial}{\partial x_2}u_1^{\text{eff}}(x_1,0) + \frac{\partial}{\partial x_1}u_2^{\text{eff}}(x_1,0)\Big)dx_1 = \frac{1}{L_1}\int_S \frac{1}{2}\nu\frac{\partial}{\partial x_2}u_1^{\text{eff}}(x_1,0). \tag{13}$$

The last equation holds because we know that the Couette flow depends only on x_2 and not on x_1.
The main issue of this work is to solve the following optimization problem: Minimize the effective tangential drag force acting on the artificial smooth boundary S

$$\min_{\gamma\in G} \quad \mathcal{F}_t^{\text{eff}} = \frac{1}{L_1}\int_S \nu\frac{\partial}{\partial x_2}u_1^{\text{eff}}(x_1,0)dx_1 \tag{14}$$

subject to the effective Couette-Navier Flow (8), which describes the homogenized flow in the viscous sublayer of a turbulent flow over microstructures. G is the set of all admissible shapes of microstructures Γ, given by $G = \{\gamma \in C^2 : [0,1] \to [-1,-0.5] \quad \big|\gamma(0) = \gamma(1) = -1, \quad \gamma(0.5) = -0.5\}$, P is the viscous sublayer in two dimensions, Σ_2 is the upper boundary of P, where the flow velocity reaches the value U, and S is the lower boundary of P, the so-called artificial smooth boundary, where the Navier Slip condition holds.
If we insert the solution of the effective Couette flow from Proposition 3 in the formula for the effective tangential drag, we get

$$\mathcal{F}_t^{\text{eff}} = \frac{\nu}{L_2}\frac{U}{1-\frac{\varepsilon}{L_2}C^{\text{bl}}}, \tag{15}$$

and following error approximation holds:

Theorem 5 *Let the skin friction $\mathcal{F}_t^\varepsilon$ be defined by (12). Then*

$$|\mathcal{F}_t^\varepsilon - \mathcal{F}_t^{eff}| \le C\varepsilon^2\frac{U^2}{\nu L_2}(1+\frac{\nu}{L_2 U}). \tag{16}$$

The formula (15) is of great impact in the theory of flows over rough surfaces. It says that the presence of any periodic roughness diminishes the tangential drag, because C^{bl} is negative and thus $\{I - \frac{\varepsilon}{L_2}C^{\text{bl}}\}^{-1} < I^{-1}$.
Being able to solve the effective equations analytically, we can do a few simplifications that have significant impact on our optimization problem. As we see in (15), our calculations are reduced to the determination of the so-called Navier constant C^{bl}. In our resulting optimization problem we only need to solve the boundary layer equation, no longer the Navier Stokes equation, which is of less computational effort:

$$\min_{\gamma\in \text{G}} \quad \text{J}(\gamma,\beta^{\text{bl}}) = \ \text{C}_\lambda^{\text{bl}} = -\int_{\text{Z}^{\text{bl}}} |\nabla\beta^{\text{bl}}(\text{y})|^2 \text{dy} \tag{17}$$

subject to the boundary layer equation

$$\begin{cases} \Delta\beta^{\text{bl}} + \nabla\omega^{\text{bl}} &= 0, \quad Z^+ \cup (Y - b_2e_2) \\ \text{div}\ \ \beta^{\text{bl}} &= 0, \quad Z^{\text{bl}} \\ \big[\beta^{\text{bl}}\big]_S(\cdot,0) &= 0, \quad S \\ \big[\{\nabla\beta^{\text{bl}} - \omega^{\text{bl}}I\}e_2\big]_S(\cdot,0) &= e_1, \quad S \\ \beta^{\text{bl}} &= 0, \quad (\gamma - b_2e_2) \\ \{\beta^{\text{bl}},\omega^{\text{bl}}\} \qquad x_1 &- \text{periodic}, \end{cases} \tag{18}$$

where $S = (0,1)$, $Z^+ = (0,1)\times(0,\infty)$, and $Z^{\text{bl}} = Z^+ \cup S \cup (Y - b_2e_2)$.
Let $V = \{z \in L^2_{loc}(Z_{bl})^2 : \nabla_y z \in L^2(Z^{\text{bl}})^4;\ z = 0 \text{ on } (\Gamma - b_2e_2);\ div_y z = 0 \text{ on } Z_{bl};\ z\ y_1 \text{ - periodic}\}$. Using test functions from this space we get the following weak formulation of the problem:

$$\beta^{\text{bl}} \in V : \int_{Z^{\text{bl}}} \nabla\beta^{\text{bl}}\nabla\varphi = -\int_S \varphi e_1 \quad \forall\varphi \in V. \tag{19}$$

Proposition 6 *Problem (19) has a unique solution $\beta^{bl} \in V$. Furthermore, there exists $\omega^{bl} \in L^2_{loc}(Z^{bl})$ such that (19) holds in the sense of distributions. Finally, $\{\beta^{bl}, \omega^{bl}\} \in V \cap C^\infty(Z^+ \cup (Y - b_2 e_2))^2 \times C^\infty(Z^+ \cup (Y - b_2 e_2))$.*

Proof. see [6]
In our boundary layer cell we defined the tip of the admissible shapes at $x_2 = -0.5$ and the artificial smooth boundary S at $x_2 = 0$. To evaluate the drag directly on the tip of the microstructures we have to translate S by 0.5.

Theorem 7 *The effective tangential drag force measured directly on the tip of the microstructures is given by*

$$\mathcal{F}_t^{\text{eff,a}} = \frac{\nu}{L_2}\Big[1 - \frac{\varepsilon}{L_2} C^{\text{bl}}\Big]^{-1} U. \tag{20}$$

and the tangential drag for the smooth surface is in this case

$$\mathcal{F}_t^{\text{smooth}} = \frac{\nu U}{L_2 + 0.5\varepsilon}. \tag{21}$$

Proof. The derivative of the linear function u^{eff} remains the same, L_2 has to be replaced by $L_2^{\text{a}} = L_2 + \frac{1}{2}\varepsilon$ and C^{bl} by $C^{\text{bl,a}} = C^{\text{bl}} - 0.5$:

$$\mathcal{F}_t^{\text{eff,a}} = \frac{\nu}{L_2 + \frac{1}{2}\varepsilon}\Big[1 - \frac{\varepsilon}{L_2 + \frac{1}{2}\varepsilon} C^{\text{bl,a}}\Big]^{-1} U = \frac{\nu}{L_2}\Big[1 - \frac{\varepsilon}{L_2} C^{\text{bl}}\Big]^{-1} U. \tag{22}$$

For the smooth plate the same considerations hold: by moving the interface downwards by $\frac{1}{2}\varepsilon$ we have to add this amount to the boundary layer thickness L_2 and we obtain (21).

□

Theorem 8 *If we compare the smooth surface with the same surface where holes are drilled in,*

$$\mathcal{F}_t^{\text{eff}} < \mathcal{F}_t^{\text{smooth}}. \tag{23}$$

Proof.

$$\frac{\nu}{L_2}\Big[1 - \frac{\varepsilon}{L_2} C^{\text{bl}}\Big]^{-1} U < \frac{\nu U}{L_2 + 0.5\varepsilon} \iff \frac{1}{L_2 - \varepsilon C^{\text{bl}}} < \frac{1}{L_2 + \frac{1}{2}\varepsilon} \iff -\varepsilon(C^{\text{bl}} + \frac{1}{2}) > 0, \tag{24}$$

which is true because the paranthesis is always negative.

For further calculations we keep the height of the microstructure $h = 0.5$ fix and minimize C^{bl}. □

5. Optimal Design Problem

Our shape optimization problem (17),(18) is a typical one in fluid mechanics. The solution $\gamma^* \in G$ satisfies $J(\gamma^*, \tilde{\beta}^{\text{bl}}(\gamma^*)) \leq J(\gamma, \beta^{\text{bl}})\ \forall \gamma \in G$. To solve an optimization problem two properties are important for the solution to the state problem: the continuity in the design variables and the differentiablility with respect to the design variables (and control variables). The discipline in optimization which deals with such information is the sensitivity analysis. From results obtained here we are able to derive the necessary optimality conditions and to describe the change in geometry.

5.1. Sensitivity Analysis

We describe the change in geometry as a normal variation of the domain. Let Γ be a part of the boundary of the domain Ω and Γ_λ respectively the part of the boundary of Ω_λ with $\Gamma_\lambda = \{s + \lambda\alpha(s)n(s) |\ s \in \Gamma\}$.

Theorem 9 *If $\beta^{bl} \in H^2(Z^{bl})$, $\alpha \in C^2([0,1])$ and small, then the change in the cost function is*

$$\delta\mathcal{J} = \int_\Gamma \alpha(s)|\partial_n \beta^{bl}(s)|^2 ds + o(||\alpha||_{C^2[0,1]}), \tag{25}$$

where $\partial_n \beta^{bl}$ is the derivative of the speed distribution, the weak solution of the boundary layer equation (18), along the outward normal n to Γ.

Before proving this theorem, we have to specify the variation of the cost function in the following way:

$$\delta\mathcal{J} = \mathcal{J}(\widetilde{Z^{\rm bl}}) - \mathcal{J}(Z^{\rm bl}) = \int_{Z^{\rm bl}} |\nabla\beta^{\rm bl}|^2 - \int_{\widetilde{Z^{\rm bl}}} |\nabla\widetilde{\beta^{\rm bl}}|^2, \tag{26}$$

where $\beta^{\rm bl}$ is the solution of the boundary layer problem in the domain $Z^{\rm bl} = Z^+ \cup S \cup (Y - b_2e_2)$ and $\widetilde{\beta^{\rm bl}}$ is the solution of the boundary layer problem in the domain $\widetilde{Z_{bl}} = Z^+ \cup S \cup (\tilde{Y} - b_2e_2)$, where $Y = \{y \in Z| \quad b_2 > y_2 > max\{0, \gamma(y_1)\}\}$, $\tilde{Y} = \{y \in Z| \quad b_2 > y_2 > max\{0, \tilde{\gamma}(y_1)\}\}$ and $\tilde{\gamma}(y_1) = \gamma(y_1) + \alpha(s)n(s)$.
We can extend $\beta^{\rm bl}$ in the domain $\widetilde{Z^{\rm bl}} \setminus (Z^{\rm bl} \cap \widetilde{Z^{\rm bl}})$ and $\widetilde{\beta^{\rm bl}}$ in $Z^{\rm bl} \setminus (Z^{\rm bl} \cap \widetilde{Z^{\rm bl}})$ by zero (see [8]). Further we denote the difference of the two solutions by $\delta\beta^{\rm bl} = \widetilde{\beta^{\rm bl}} - \beta^{\rm bl}$, where $\delta\beta^{\rm bl} \in Z^{\rm bl} \cup \widetilde{Z^{\rm bl}}$, and $\delta Z^{\rm bl} = Z^{\rm bl} \setminus (Z^{\rm bl} \cap \widetilde{Z^{\rm bl}}) - \widetilde{Z^{\rm bl}} \setminus (Z^{\rm bl} \cap \widetilde{Z^{\rm bl}})$, which is a very small domain.

Lemma 10 *$\delta\beta^{bl}$ is the solution of the following system:*

$$\begin{cases} -\Delta_y\delta\beta^{bl} + \nabla_y\delta\omega^{bl} &= 0, \text{ in } Z^{bl} \\ \operatorname{div}_y\ \delta\beta^{bl} &= 0, \text{ in } Z^{bl} \\ \left[\delta\beta^{bl}\right]_S(\cdot,0) &= 0, \text{ auf } S \\ \left[\{\nabla_y\delta\beta^{bl} - \delta\omega^{bl}I\}e_2\right]_S(\cdot,0) &= 0, \text{ auf } S \\ \delta\beta^{bl} &= -\alpha\partial_n\beta^{bl}, \text{ auf } (\gamma - b_2e_2) \\ \{\delta\beta^{bl}, \delta\omega^{bl}\} \quad (y_1) &- \text{ periodic,} \end{cases} \tag{27}$$

Proof. The only non-obvious relation is the boundary condition on $(\gamma - b_2e_2)$. We get it using the Taylor expansion for $\widetilde{\beta^{\rm bl}} = 0$ on $\tilde{\Gamma}$ and the fact that $\partial_n\widetilde{\beta^{\rm bl}}(x)\big|_\Gamma$ is weakly continuous in α.

□

Proof. (of the theorem) With these assumptions we can transform the variation of the object function:

$$\begin{aligned} \delta\mathcal{J} &= \mathcal{J}(\widetilde{Z^{\rm bl}}) - \mathcal{J}(Z^{\rm bl}) = \textstyle\int_{Z^{\rm bl}} |\nabla\beta^{\rm bl}|^2 - \int_{\widetilde{Z^{\rm bl}}} |\nabla(\beta^{\rm bl} + \delta\beta^{\rm bl}|^2 \\ &= -\textstyle\int_{\delta Z^{\rm bl}} |\nabla\beta^{\rm bl}|^2 - 2\int_{Z^{\rm bl}} \nabla\beta^{\rm bl}\nabla\delta\beta^{\rm bl} + o(\delta Z^{\rm bl}, \delta\beta^{\rm bl}). \end{aligned} \tag{28}$$

Now we calculate the two terms in the above equation separately. To the first term we apply a change in coordinates and the mean value theorem for integration:

$$\int_{\delta Z^{\rm bl}} |\nabla\beta^{\rm bl}|^2 = \int_0^\alpha \int_\Gamma |\nabla\beta^{\rm bl}|^2 + o(||\alpha||_{C^2}) = \int_\Gamma \alpha|\partial_n\beta^{\rm bl}|^2 + o(||\alpha||_{C^2[0,1]}). \tag{29}$$

For the second term we use the corresponding boundary layer equation which in this case is self-adjoint, the corresponding boundary values, partial integration and the incompressibility:

$$\begin{aligned} \textstyle\int_{Z^{\rm bl}} \nabla\beta^{\rm bl}\nabla\delta\beta^{\rm bl} &= \textstyle\int_{Z^{\rm bl}}(-\Delta\beta^{\rm bl})\delta\beta^{\rm bl} + \int_{\partial Z^{\rm bl}}(\partial_n\beta^{\rm bl})\delta\beta^{\rm bl} \\ &= \textstyle\int_\Gamma(\partial_n\beta^{\rm bl} - \omega^{\rm bl}n)(-\alpha(\partial_n\beta^{\rm bl})) = -\int_\Gamma \alpha|\partial_n\beta^{\rm bl}|^2. \end{aligned} \tag{30}$$

Adding these two integrals we obtain (25).

□

5.2. Optimality Condition
On the basis of the previous results we can now formulate necessary optimality conditions satisfied by optimal solutions. Their interpretation may reveal some important properties and may give a hint how to choose the geometry deformation.
Let $\mathcal{O} = \{\Omega \quad \big| \quad \Omega = Z^{\rm bl}, \text{ with } \gamma \in G, \text{ where } \gamma \subset \partial\Omega\}$.

Theorem 11 *If the solution of (17),(18) is smooth, it satisfies the necessary condition*

$$|\partial_n\beta^{bl}|^2 = \text{const} \quad \text{on} \quad \Gamma. \tag{31}$$

Proof. If the domain $\Omega \in \mathcal{O}$ is optimal, with Γ being the part of the boundary which describes the shape of the roughness, then $\delta\mathcal{J} = 0$ holds for every admissible α. Thus, inserting the results of the previous theorem, and by the well known Lagrange multiplier rule, there exists a constant λ (Lagrange multiplier) such that $|\partial_n \beta^{\mathrm{bl}}|^2 = \lambda \quad \text{on} \quad \Gamma$. We say that α is *admissible*, if

$$-\int_\Gamma \alpha d\Gamma = o(||\alpha||_{C^2[0,1]}). \tag{32}$$

This is the condition by which $\Omega \in \mathcal{O}$ implies $\Omega_\alpha \in \mathcal{O}$.

□

5.6. Numerical Simulation and Results

Theorem 9 indicates how to choose α such that $J(\gamma + \alpha n, \tilde{\beta}^{\mathrm{bl}}) \leq J(\gamma, \beta^{\mathrm{bl}})$. For our optimization problem we obtain a sequence of admissible shapes if we build a shrinking sequence of humps with constant height.

For the numerical realization we have to do a few approximations. In the first step we have to approximate the infinite domain of the boundary layer problem, i.e. we have to cut it at a position $y = k$ and to impose additional boundary conditions on that part of the domain, so that the resulting finite domain describes a good approximation of the original infinite domain. On this finite domain we apply the software FEMLISP. FEMLISP was developed at IWR by N. Neuss to solve the state equation. It uses finite elements for the discretization in space. Because of the incompressibility we need a stable discretization, i.e. the Taylor-Hood element which approximates the velocity piecewise with a polynom of degree k and the pressure piecewise with a polynom of degree k-1 on the generated mesh. In our calculations we use k=4. Up to now the program deals with an interpolation error estimater, which could be improved in future. To solve the discretized problem FEMLISP can use direct solvers like UMFPACK or a multigrid solver. The multigrid solver so far runs only with uniform refinements; adaptive refinements can be implemented in future. The smoothing step uses block smoothing, a rollover subspace correction without any degrees of freedom for the pressure on the boundary. Simulations are shown in figure 1.

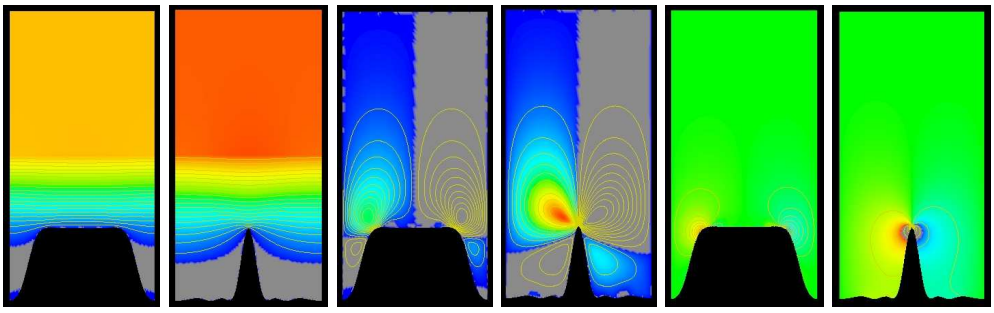

x-velocity (range: 0 – 0.6) y-velocity (range: 0 – 0.036) pressure p (range: -1.5 – 1.5)

Figure 1: *Numerical simulations of the boundary layer cell with FEMLISP (IWR, N. Neuss)*

6. The three dimensional viscous sublayer of a turbulent flow over longitudinal riblets

In the three dimensional case we have to consider longitudinal and cross flow. The longitudinal flow is the stream flow and the cross flow is generatd by the turbulent motion in the layer above the viscous sublayer. So that the correct model for the viscous sublayer is a Couette flow, deflected from the main stream velocity. The boundary condition on the top of the channel is therefore the velocity $U = (U_1, U_2, 0)$.

6.1. The protrusion height

Bechert defined in [1] the protrusion height h_p as the distance of the riblet tips from the virtual origin of the velocity profile. We denote the protrusion height of the longitudinal or parallel flow by $h_{p||}$ and

the protrusion height of the cross flow by $h_{p\perp}$. In our model this protrusion height can be associated with the Navier constant in the following way:

Definition 12 *The* protrusion height *of the parallel flow is given by*

$$h_{p||} = \varepsilon C_{||}^{bl}. \tag{33}$$

The protrusion height *of the cross flow is given respectively by*

$$h_{p\perp} = \varepsilon C_{\perp}^{bl}, \tag{34}$$

where $C_{\perp}^{bl}$ is calculated from (18) and $C_{||}^{bl}$ from the simplified Laplace equation resulting from the special geometry.

The protrusion height is a length which depends only on the choosen reference length and not upon the reference velocity. The ratio of protrusion height to the period of the corrugations, $\frac{h_p}{s}$, is called the *normalized protrusion height* $\bar{h}_p$ and depends only on the shape of the microstructures and neither on their size nor on the actual speed of he fluid. Bechert (in [2]) and Luchini (in [9]) showed before that the only parameter which the behaviour of the turbulent boundary layer depends on is the difference between the two protrusion heights $d_h = h_{p||} - h_{p\perp}$, the distance between the two virtual plane walls, where the velocity is zero, seen by the longitudinal and cross flow. We will see that the origin of the cross flow lies always higher than the one of the longitudinal flow, and thus d_h is a measure of how much the microstructures impede the cross flow more than the longitudinal flow. The higher the difference between the two protrusion heights is the greater is the contribution to the drag reduction.
We found out, that the quantitative parameter which characterizes how much the microstructures reduce drag, is the Navier constant C^{bl}. Let us calculate the normalized difference between the protrusion heights:

$$d_{\bar{h}} = \bar{h}_{p\perp} - \bar{h}_{p||} = \frac{h_{p\perp} - h_{p||}}{s} = \frac{\varepsilon(C_{\perp}^{\mathrm{bl}} - C_{||}^{\mathrm{bl}})}{\varepsilon} = C_{\perp}^{\mathrm{bl}} - C_{||}^{\mathrm{bl}}. \tag{35}$$

Luchini, Manzo and Pozzi found out in [9] that the maximum possible difference between the heights of the two origins is $d_h = 0.132s$, which means $d_{\bar{h}} = 0.132$ and $0 < C_{\perp}^{\mathrm{bl}} - C_{||}^{\mathrm{bl}} \leq 0.132$ for all possibles shapes. The optimization problem for the three dimensional case concerning both the longitudinal and the cross flow is then

$$\max_{\gamma \in G} |C_{||}^{\mathrm{bl}} - C_{\perp}^{\mathrm{bl}}| = \min_{\gamma \in G}(C_{||}^{\mathrm{bl}} - C_{\perp}^{\mathrm{bl}}), \tag{36}$$

since $C_{||}^{\mathrm{bl}} - C_{\perp}^{\mathrm{bl}} < 0$. At first glance it seems that we have to minimize the Navier constant from the longitudinal flow and maximize the Navier constant from the cross flow. But this is not possible because the two constants are connected to each other by the three dimensional geometry. Maximizing the Navier constant would mean the inverse process as done in section 5. From there we know that the worse microstructure from the cross flow is the one with a bigger cross section, with more material, smooth and flat tips. Exactly this type of microstructure dampens the cross and the longitudinal flow even more, because the valleys are too narrow. So we have to minimize both, the Navier constant from cross flow and the Navier constant from the longitudinal flow. Then the difference between them gets greater.

6.2. Numerical results for the cross and longitudinal flow
In this subsection we apply results of the two dimensional calculations to the cross flow, compare the non-optimized with the optimized microstructure and analyse the effect on the corresponding longitudinal flow.
The starting shape (see figure 2) gives us the following Navier constants: $C_{\perp}^{\mathrm{bl}} = -0.514$ and $C_{||}^{\mathrm{bl}} = -0.5280$. The normalized difference of the protrusion heights is thus $d_{\bar{h}} = 0.014$. The optimized shape (see figure 3) gives us the following numbers: $C_{\perp}^{\mathrm{bl}} = -0.580$, $C_{||}^{\mathrm{bl}} = -0.68855$ and $d_{\bar{h}} = 0.1086$. For a thinner peak (see figure 4) we get $C_{\perp}^{\mathrm{bl}} = -0.582$, $C_{||}^{\mathrm{bl}} = -0.69898$ and $d_{\bar{h}} = 0.117$. We see again that the slit is the optimum in this case with following values: $C_{\perp}^{\mathrm{bl}} = -0.582$, $C_{||}^{\mathrm{bl}} = -0.7$ and $d_{\bar{h}} = 0.118$.
Now, we would like to evaluate the effect of the microstructures on the drag. Herefor we compare the drag force for the different structures:

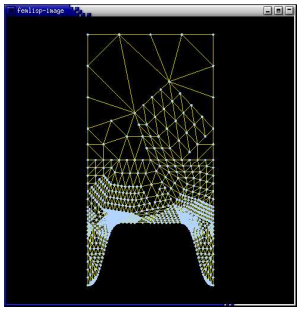

Figure 2: *mesh of order 3 of the starting shape*

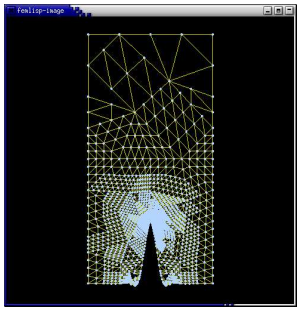

Figure 3: *mesh of order 3 of the shape optained from the optimization process*

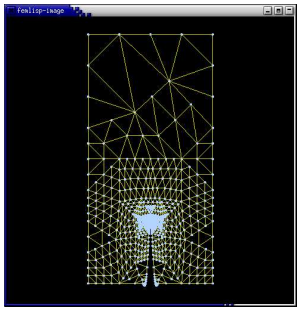

Figure 4: *mesh of order 3 of a thinner peak*

Theorem 13 *The effective tangential drag force measured on the tip of the microstructures is given by*

$$\mathcal{F}_{\mathrm{t},1}^{\mathrm{eff}} = \frac{\nu}{L_3}\Big[1 - \frac{\varepsilon}{L_3}C_{||}^{\mathrm{bl}}\Big]^{-1}U_1,$$

$$\mathcal{F}_{\mathrm{t},2}^{\mathrm{eff}} = \frac{\nu}{L_3}\Big[1 - \frac{\varepsilon}{L_3}C_{\perp}^{\mathrm{bl}}\Big]^{-1}U_2,$$

and the tangential drag for the smooth surface is in this case

$$\mathcal{F}_{\mathrm{t},1}^{\mathrm{smooth}} = \frac{\nu U_1}{L_3 + 0.5\varepsilon},$$

$$\mathcal{F}_{\mathrm{t},2}^{\mathrm{smooth}} = \frac{\nu U_2}{L_3 + 0.5\varepsilon}.$$

For $\varepsilon = 3 \cdot 10^{-4}m$ we have $\mathcal{F}_{\mathrm{t},1}^{\mathrm{smooth}} = 0.8696 \cdot 10^{-6}$, $\mathcal{F}_{\mathrm{t},2}^{\mathrm{smooth}} = 0.8696 \cdot 10^{-6}$ and $\mathcal{F}_{\mathrm{t},1}^{\mathrm{eff}} = 0.8267 \cdot 10^{-6}$, $\mathcal{F}_{\mathrm{t},2}^{\mathrm{eff}} = 0.8514 \cdot 10^{-6}$. Thus $|\mathcal{F}_t^{\mathrm{smooth}}| = 1.2298$ and $|\mathcal{F}_t^{\mathrm{eff}}| = 1.1867$, which is 3.5% better than in the case of the smooth structure. Further calculations are colected in table 1.

Table 1: effect of the height of the microstructure on the skin friction

$h \cdot 10^{-4}$	$\frac{\varepsilon}{\delta}$	$\lvert\mathcal{F}_t^{\mathrm{smooth}}\rvert$	$\lvert\mathcal{F}_t^{eff}\rvert$ non-optimized (%)	$\lvert\mathcal{F}_t^{eff}\rvert$ optimized (%)
0.25	0.05	1.3797	1.3783 (0.1%)	1.3703 (0.7%)
0.5	0.10	1.3469	1.3442 (0.2%)	1.3291 (1.3%)
0.75	0.15	1.3155	1.3117 (0.3%)	1.2904 (1.9%)
1.0	0.20	1.2856	1.2807 (0.38%)	1.2538 (2.5%)
1.5	0.30	1.2297	1.2230 (0.54%)	1.1867 (3.5%)
2.0	0.40	1.1785	1.17035 (0.7%)	1.12637 (4.4%)
2.5	0.50	1.1314	1.1219 (0.8%)	1.0719 (5.3%)
3.0	0.60	1.0878	1.0774 (1%)	1.0226 (6%)

7. Conclusion

We have seen that homogenization theory facilitates our numerical computations of physical phenomena in which microscopic irregularities arise. The macroscopic (averaged) model is derived by describing the limiting behaviour (where the period tends to zero) of the solutions of an elliptic boundary value problem with periodic coefficients. These effective equations have smooth coefficients and solutions. Deriving the effective solutions analytically was of great impact to our optimization problem since the efforts of

computations are reduced. With these considerations we were able to explain the influence of the shape of riblets on the viscous sublayer of a turbulent flow, as laboratories have examined in experiments. The most important contribution of the microstructures to the drag minimization seems to be that the cross flow is dampened compared to the smooth case which has effect that the vorticities in the buffer layer get narrower. In future, analysis and also direct simulations of turbulent flow have to be taken into account in this context.

8. Acknowledgement
The presented results are a part of my PhD thesis (see [4]) at the University of Heidelberg supervised by Professor W. Jäger and supported by the International Graduiertenkolleg, IGK 710 "Complex processes: Modeling, Simulation, and Optimization". My considerations are based on the work of Prof. W. Jäger (University of Heidelberg) and Prof. A. Mikelić (University of Lyon) in homogenization (see [6]).

References

[1] D.W. Bechert, M. Bartenwerfer, and W.-E. Hoppe, G.and Reif. Drag reduction mechanisms derived from shark skin. *AIAA, In 15th Congr. Intl. Counc. Aeronautical Science*, London, September 7-12:1044–1068, 1986.

[2] D.W. Bechert, M. Bruse, W. Hage, J.G.T. van der Hoeven, and G. Hoppe. Experiments on drag-reducing surfaces and their optimization with an adjustable geometry. *J. Fluid Mech.*, 338:59–87, 1997.

[3] D.W. Bechert and W.-E. Hoppe, G.and Reif. On the drag reduction of the shark skin. *AIAA, Shear Flow Control Conference*, Boulder (Colorado), March 12-14:1–18, 1985.

[4] E.. Friedmann. *Shape optimization on microstructures - the theory of riblets in the viscous sublayer.* University Heidelberg, PhD thesis to appear in 2005.

[5] W. Jäger and A. Mikelić. On the roughness-induced effective boundary conditions for a viscous flow. *Journal of Differential Equations*, 170:96–122, 2001.

[6] W. Jäger and A. Mikelić. Couette flows over a rough boundary and drag reduction. *Communications in Mathematical Physics*, 232:429–455, 2003.

[7] W. Jäger, A. Mikelić, N. Neuß, and G. Hoppe. Asymptotic analysis of the laminar viscous flow over a porous bed. *Communications in Mathematical Physics*, 232:429–455, 2003.

[8] O. Ladyzhenskaya. *The mathematical theory of viscous incompressible flow.* Gordon Breach, 1963.

[9] P. Luchini, F. Manzo, and A. Pozzi. Resistance of a grooved surface to parallel flow and cross-flow. *J. Fluid Mech.*, 228:87–109, 1991.

[10] B. Mohammadi and O. Pironneau. *Applied Shape Optimization for Fluids.* Oxford University Press, Oxford New York, 2001.

[11] N. Neuß. Femlisp - a toolbox for solving partial differential equations with finite elements and multigrid. *SFB-Preprint*, 2003.

[12] O. Pironneau. On optimum profiles in stokes flow. *J. Fluid Mech.*, 59:117–128, 1973.

[13] O. Pironneau. On optimum design in fluid mechanics. *J. Fluid Mech.*, 64:97–110, 1974.

[14] O. Pironneau. *Optimal Shape Design for Elliptic Systems.* Springer-Verlag, New York, 1984.